

## Modified electrolyte leakage method for testing the oxidative stability of *Pinus mugo* Turra under ozone-induced stress

Svetlana Bičárová<sup>1\*</sup>, Veronika Lukasová<sup>1</sup>, Katarína Adamčíková<sup>2</sup>,  
Lucia Žatková<sup>3</sup>, Rastislav Milovský<sup>3</sup>, Anumol Shashikumar<sup>4</sup>, Jozef Pažitný<sup>2</sup>,  
Anna Buchholcerová<sup>1,5</sup>, Dušan Bilčík<sup>1</sup>

<sup>1</sup>Earth Science Institute of the Slovak Academy of Sciences, Stará Lesná,  
059 60 Tatranská Lomnica, Slovakia

<sup>2</sup>Department of Plant Pathology and Mycology, Institute of Forest Ecology  
of the Slovak Academy of Sciences, Akademická 2, 949 01 Nitra, Slovakia

<sup>3</sup>Earth Science Institute of the Slovak Academy of Sciences, Ďumbierska 1,  
974 11 Banská Bystrica, Slovakia

<sup>4</sup>Groupe International d'Etudes des Forêts Sud-européennes G.I.E.F.S,  
69, Avenue des Hespérides, 06300 Nice, France

<sup>5</sup>Faculty of Mathematics, Physics and Informatics, Comenius University,  
Mlynská dolina F1, 841 48 Bratislava, Slovakia

### Abstract

BIČAROVÁ, S., LUKASOVÁ, V., ADAMČIKOVÁ, K., ŽATKOVÁ, L., MILOVSKÝ, R., SHASHIKUMAR, A., PAŽITNÝ, J., BUCHHOLCEROVÁ, A., BILČÍK, D., 2023. Modified electrolyte leakage method for testing the oxidative stability of *Pinus mugo* Turra under ozone-induced stress. *Folia Oecologica*, 50 (1): 1–15.

Electrolyte leakage (EL) is the method commonly used to test the cell membrane integrity of plants under stress conditions. The cells of the leaf may be damaged by ozone ( $O_3$ ) entering the intercellular space as an oxidative stress agent. The modified EL method was used to test the oxidative stability (OxS) of plant tissue against  $O_3$ -induced oxidative stress. The modification includes simulation of the artificial oxidative stress by additional ozonation of plant samples in the laboratory chamber. This modified EL method was applied to *Pinus mugo* Turra needle samples collected in the subalpine zone of the High Tatra Mts (Western Carpathians), in the years 2019 and 2020. Changes in the chemical composition of samples after artificial ozonation were traced by gas chromatography/mass spectrometry (GC/MS) analysis. In addition,  $O_3$  uptake through open stomata was estimated by calculation of the modelled ozone dose ( $MO_3D$ ). We also conducted an inspection of visible injury (VIN) on the needle surface focused on the occurrence of  $O_3$ -induced symptoms and biotic harmful agents. Regarding OxS results as well as VIN indices, *P. mugo* needles showed relatively low sensitivity to oxidative stress induced by  $O_3$ . Therefore  $MO_3D$  in a range between 14 and 16  $mmol\ m^{-2}$  can be considered as  $O_3$  dose with minor phytotoxic effect on *P. mugo* growing in the mountains of central-eastern Europe.

### Keywords

cell membrane integrity, injury index, modelled ozone dose, mountain environment, ozone, visible injury

\*Corresponding author:

e-mail: svetlana.bicarova@savba.sk

©2023 Authors. This is an open access article under the CC BY-NC-ND license (<http://creativecommons.org/licenses/by-nc-nd/4.0/>)

## Introduction

Ozone ( $O_3$ ) in ambient air is considered as an anthropogenic stress factor acting on terrestrial vegetation (LICHTENTHALER, 1996) including the land areas covered by forests (BRAUN et al., 2017; BYTNEROWICZ et al., 2019; HŮNOVÁ et al., 2019; ZAPLETAL et al., 2012). Current air quality standards for forests such as exposure index (AOT40) and phytotoxic ozone dose (POD) indicate a high risk of ozone damage in the mountain regions (Bičárová et al., 2019; EMEP, 2020). These ozone metrics are based on measured  $O_3$  concentration and modelled abiotic environmental factors. Besides that, ozone-sensitive species typically exhibit foliar injury that can be visually diagnosed in the field (DALSTEIN and CIRIANI, 2019). *Pinus* species are on the list of plant species that are known to respond negatively to high  $O_3$  exposure (BELL et al., 2020) by injury such as chlorotic mottling, which is visible on the surface of the needles. However, the response to  $O_3$  injury under actual conditions may vary in dependence on  $O_3$  sensitivity controlled by genotype and microsite conditions of growth, exposure, and stomatal  $O_3$  flux (COULSTON et al., 2003; NUNN et al., 2007). The development of visible injury (VIN) including  $O_3$ -induced traces is inter- and intra-species specific, and also depends on other environmental biotic and climatic factors. Due to the complex nature of the diagnosis, inspection of visible injury is regarded to be the semi-quantitative method for the assessment of ozone damage on forest trees (SCHAUB et al., 2016).

Stress conditions and stress-induced damage in plants can be detected using the classical eco-physiological methods such as measuring the rates of photosynthesis, respiration and transpiration, the stomatal conductance and water potential, as well as content and ratios of the photosynthetic pigments (chlorophylls and carotenoids) or the concentration of stress metabolites (LICHTENTHALER, 1996). A revolutionary breakthrough in understanding the abiotic stress-tolerance mechanisms brought mapping quantitative trait loci (QTL) (SALLEM et al., 2020). In the previous studies (e. g. FLINT et al., 1967), an electrolytic method was used to derive the index of injury referring to stress. The electrolyte leakage (EL) became the commonly used assay to measure the plant tissue response to stress factors (LEVITT, 1972; PENNAZIO and SAPETTI, 1982; BAJJI et al., 2002; LEE and ZHU, 2010; ESCANDÓN et al., 2016). The stress-induced EL is usually accompanied by the accumulation of reactive oxygen species (ROS) related to  $K^+$  efflux from plant cells, which is mediated by plasma membrane cation conductance (DEMIDCHIK et al., 2014). Lipids play a crucial role in determining cell structures regulating membrane fluidity and transducing signals (FURT et al., 2011). Severe oxidation of lipids produces highly reactive lipid peroxidation-derived molecules that can cause irreversible damage in plant cells, which ultimately leads to cell death (YALCINKAYA et al., 2019).

This article focuses on mountain pine (*Pinus mugo* Turra), the dominant vegetation of the subalpine

zone in the Western Carpathians where harsh mountain environment is affected by the action of changing climate conditions, the higher  $O_3$  exposition, and other biotic and abiotic stress agents (BADEA et al., 2004; FLEISCHER et al., 2017; KOPÁČEK et al., 2017; MEZEI et al., 2017). We assume that the application of EL method on plant material will allow us to estimate membrane injury caused by oxidative stress. In this study, we were particularly conducted in the application of EL method modified for testing ozone-induced injury effect on plant tissue of *P. mugo* affected by relatively high  $O_3$  concentration in the natural environment. The modification includes additional artificial ozonation of needle samples exposed to extremely high  $O_3$  concentrations in the laboratory chamber. It is expected that gas chromatography/mass spectrometry (GC/MS) analysis may detect changes of the chemical composition in lipid fraction of needle samples. Results based on the modified EL method together with inspection of visible injury should be useful for classification of phytotoxicity effect of ozone dose received by *P. mugo* from ambient air in the natural conditions.

The objectives of this work were: (i) to use the modified EL method for testing the sensitivity of *P. mugo* cell membranes on oxidative stress; (ii) to analyse the chemical composition of the lipid fraction in needle samples and leachates after the EL procedure by GC/MS analysis; (iii) to determine the value of oxidative stability (OxS) and to scale range of the visible injury (VIN) for *P. mugo* samples collected in the High Tatra Mts (Slovakia) at the start and at the end of the growing season in the years 2019 and 2020; (iv) to classify the phytotoxic effect of modelled ozone dose ( $MO_3D$ ) up-taken by *P. mugo* under actual environmental conditions using OxS and VIN indicators.

## Materials and methods

### Plant material and experimental design

In testing of ozone-induced effect on plant material, we selected *P. mugo* as the dominant vegetation species of subalpine belt between 1,600 to 2,200 m asl in the High Tatra Mts, Slovakia (Fig. 1). *Pinus mugo* growing in this high mountain region is exposed to relatively high ambient  $O_3$  concentration in environmental conditions, that support the stomatal  $O_3$  flux into cells (Bičárová et al., 2019). It is typical mountain vegetation widespread over the timberline that forms pure scrubland communities of shrubs with many spreading stems – polycormones, and dense, two-needle shoots. The needle lifecycle span is about 5–6 years with the altitude-dependent prolongation (BORATYŃSKI et al., 2009). Among the other European pines, *P. mugo* is the most tolerant to cold climates and to bedrock lithology, adapted to any rocky habitat in the high-altitude mountains of Europe (BALLIAN et al., 2016). In the vicinity of Skalnaté Pleso Observatory, where the regular meteorological and  $O_3$  measurements have started in 1943 and 2000, respectively, ten monitoring sites

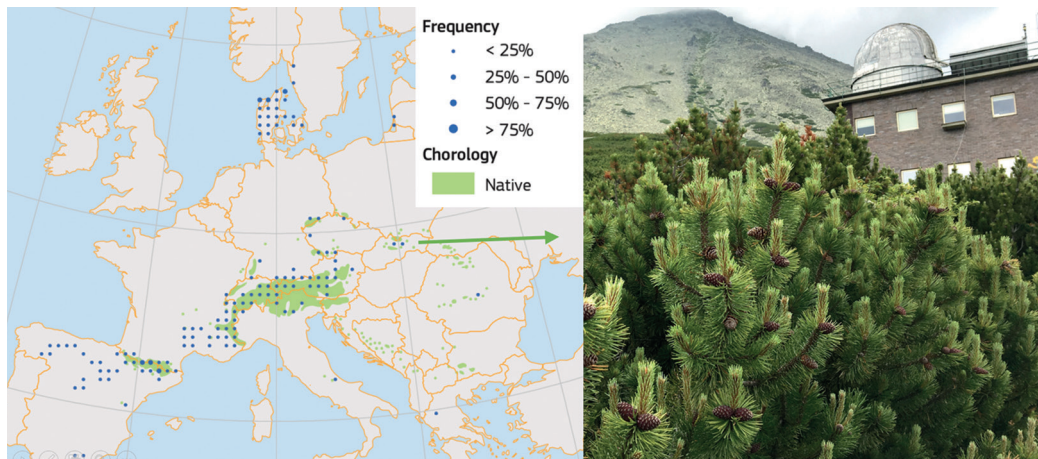


Fig. 1. Spatial distribution of *P. mugo* in Europe (BALLIAN et al., 2016) – left; image in right illustrates *P. mugo* in the vicinity of Skalnaté Pleso Observatory in the High Tatra Mts, Slovakia.

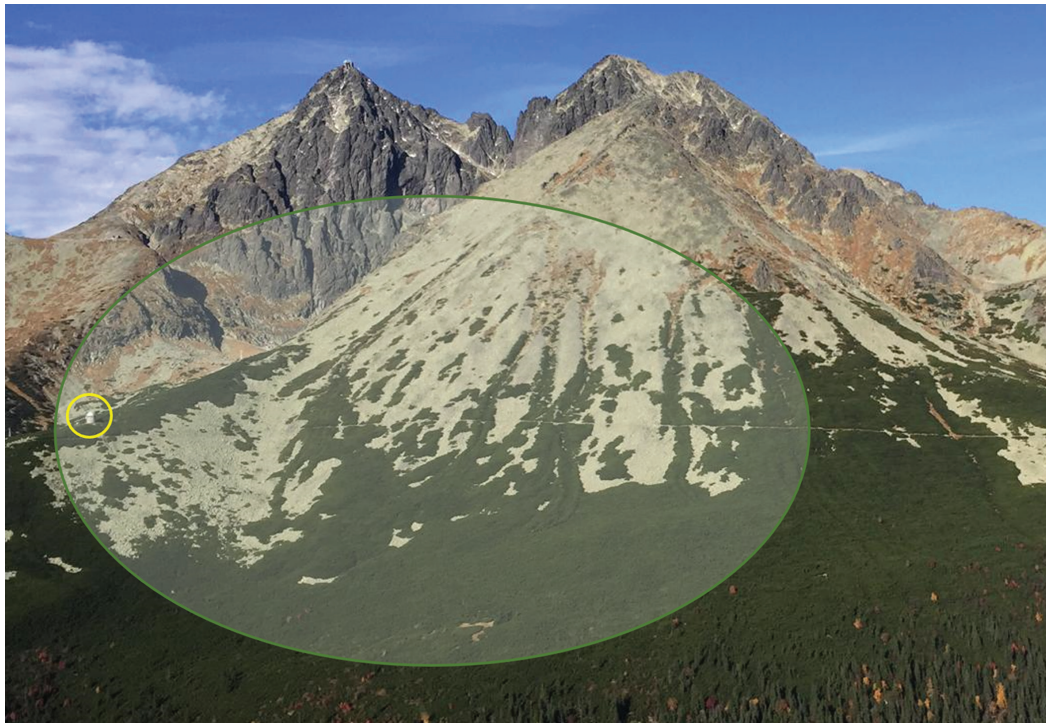


Fig. 2. Sample collection area of *P. mugo* needle in High Tatra Mts (green ellipse); yellow circle marks the position of Skalnaté Pleso Observatory (Lat 49°11'21.86"N, Long 20°14'02.38"E, Alt 1,778 m asl).

(S1–S10) were established for the collection of *P. mugo* needle samples (Fig. 2). The density of *P. mugo* thickets decreases with increasing altitude. In our experiment, three shrubs at each of S1–S6 sites at lower altitudes between 1,600 and 1,900 m asl were selected. While at higher altitudes of 2,000 m asl, where only the single shrubs occur, one shrub at each S7–S10 position was selected. One branch of each shrub was permanently marked by a plastic tap. At each branch, we differentiated 2-year-old (C + 2) needles on which the O<sub>3</sub> injury is most pronounced (BIČÁROVÁ et al., 2019). About 10 twin needles were carefully pulled and wrapped in aluminium foil placed in a small plastic zip-lock bag. Needle samples were on the same day transported to the laboratory and stored in the refrigerator. The laboratory procedures were performed

on next day. The field experiment started in June 2019. The field sampling collection was repeated on the same branches in October 2019 and in the following year 2020 in similar terms i.e. at the beginning of June, and early October.

#### Visible foliar injury

Laboratory procedures began by the inspection of 2-year-old (C + 2) needles collected at the monitoring sites (S1–S10). Needle samples were inspected under the magnifying glass for injuries visible on their surface. The visible injury (VIN) was differentiated for the following three stress factors:

- i) VINbio – biotic diseases including the impact of biotic agents such as stinging insect, spider mites

- (Fig. 3a), and fungi (Fig. 3b),
- ii) VINabio – abiotic damage primarily due to mechanical effect (Fig. 3c),
  - iii) VINO<sub>3</sub> – ozone-induced injury (Fig. 4).



Fig. 3. Examples of visible foliar injury on *P. mugo* surface of 2-year-old (C + 2) needles collected at the monitoring sites in the High Tatra Mts: a) necrotic tissue primarily caused by insects, spider mites; b) fungi; c) abiotic-mechanical damage.

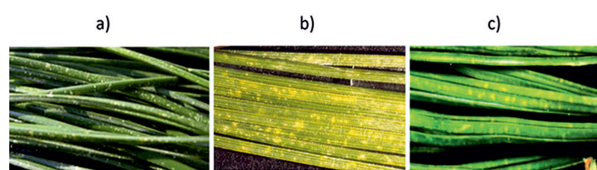


Fig. 4. Foliar ozone symptoms on the needles of a) *Pinus cem-bra* (DALSTEIN and CIRIANI, 2019); b) *Pinus halepensis* (ICP, 2014); c) *Pinus strobus* (SHARPS et al., 2014).

Ozone sensitive species exhibit foliar symptoms such as mottling that occurred as a small spot of yellow/light green or mottling with a diffuse outline, especially on the upper surface and at the tip of the needles (Fig. 4). The development of spots on the needle due to ozone damage can be followed by leaf chlorosis (yellowing or paling of green plant tissue), (ICP, 2014).

VIN on *P. mugo* was scored for each sample according to the percentage of the damaged area on the needle surface (Table 1) with respect to the classes mentioned in SCHAUB et al. (2016) for each harmful factor individually. We defined VINbio, VINabio, VINO<sub>3</sub> as the median of score for the group of samples gathered in single clusters considering for beginning and end of the growing season, separately.

Table 1. Classification of visible injury

Legend	Percentage of damage on surface needles	Score
No injury	0%	0
Low	1-5 % of the surface is affected	1
Moderate	6-50 % of the surface is affected	2
Large	51-100 % of the surface is affected	3

### Electrolyte leakage technique

In this study, we assumed that EL is directly proportional to cell membrane damage expressed as a percentage  $EL (\%) = [(C_f - C_i / C_i - C_i)] \times 100$  (Eqn. 1), where  $C_i$  is ultra-pure water conductivity at initial conditions,  $C_f$  is final conductivity of water solution after incubation of

plant material overnight at room temperature under agitation at 150 rpm on a shaker, and  $C_i$  is total conductivity of water solution after total plant material destruction in autoclave for 20 minutes at 121 °C and further cooling at room temperature for 5 hours under agitation at 150 rpm. EL conductivity was measured by calibrated conductometer TDS Testr 11 (Eutech Instrument, Thermo Fisher Scientific Inc., Singapore).

### Procedure of EL method modified to test oxidative stability of cell membranes

After the visual inspection, samples were processed under the next steps of the EL procedure.

1. The needles were cut into 1 cm long pieces by eliminating both ends, and then weighed exactly  $2 \times 100$  mg ( $1 \times 100$  mg samples for standard EL procedure and  $1 \times 100$  mg for ELO<sub>3</sub> procedure with additional artificial ozonation).
2. The weighed needles were then rinsed thrice in the 2 ml Eppendorf tubes.
3. The initial conductivity  $C_i$  was measured using 10 ml ultra-pure water in 15 ml Falcon tubes.
4. Additional ozonation was done by exposing the samples ( $1 \times 100$  mg) to artificial O<sub>3</sub> in a laboratory chamber under controlled O<sub>3</sub> input flow (Fig. 5). Ozone flux in the chamber was regulated so that the plant material was exposed to artificial O<sub>3</sub> in an amount of around 150 ppm within two hours. This O<sub>3</sub> dose corresponds to the expected cumulative amount of O<sub>3</sub> concentration in natural environment in the High Tatra Mts during the growing season. The ozonation in the laboratory chamber was also monitored by passive sensor based on the selective reaction of indigo with ozone, which is manifested by a color change from blue (indigo) to yellow (isatine, as a product of indigo oxidation reaction). After ozonation, the color change was detected on a scale that corresponds to the scale of the indigo sensor exposed in the natural environment. The ozone potentially penetrates into cellular structures by two means: through the stomatal pores, which are not air tightly closed after the sampling manipulation; through the cross-section profiles created by the cutting that allows the diffusion of O<sub>3</sub> to the interior spongy mesophyll area (Fig. 6).
5. Both the samples, artificially non-ozonized and ozonized were incubated in the Falcon tubes overnight at the room temperature under the agitation at 150 rpm on the shaker.
6. On the day 2, the final conductivity  $C_f$  of the water solution in tubes was measured.
7. All the samples in the tubes were autoclaved for 20 minutes at 121 °C and then cooled at the room temperature for 5 hours under the agitation conditions described in step 5.
8. The total conductivity  $C_i$  was measured. It is assumed that the conductivity after autoclaving represents 100% of electrolyte leakage.
9. Calculation of EL (%) was carried out using Eqn. 1.

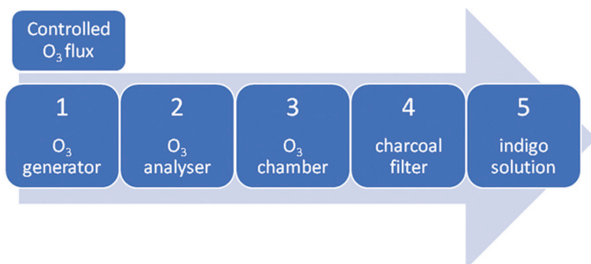


Fig. 5. Scheme of artificial ozonation process: 1 – electrochemical production of O<sub>3</sub> using Koizon 300 equipment, a product of Gemke Technik GmbH, regulation of flow rate at the level of 0.5 Lpm; 2 – measurement of O<sub>3</sub> concentration in flow between the output of O<sub>3</sub> generator and the input to the chamber by Thermo Electron Environmental 49C device; 3 – the flow chamber for ozonation of needle samples placed in a perforated Eppendorf 2 ml tubes; 4 – adsorption of O<sub>3</sub> flow by activated charcoal; 5 – absorption of O<sub>3</sub> flow in indigo solution accompanied with visible colour change.

Values EL and ELO<sub>3</sub> (%) are consistent with the following injury indices that reflect two different types of O<sub>3</sub> exposure: (i) INX, related to the ambient O<sub>3</sub> exposure in the natural environment i.e. samples artificially non-ozonized, and (ii) INXO<sub>3</sub> for samples exposed to additional ozonation in laboratory chamber.

To investigate the differences in injury indices between additionally ozonized (INXO<sub>3</sub>) and non-ozonized (INX) samples of *P. mugo* needles gathered in individual months (June, October) and years (2019, 2020) paired samples t-test in software Statistica was used. The null hypothesis of no differences between the samples was rejected at  $p < 0.05$  and indicate significant differences.

### Gas chromatography/mass spectrometry (GC/MS)

Quantitative and qualitative analysis of the total lipid extract (TLE) from dried needle samples as well as TLE from water leachates after EL procedure were performed by GC/MS (gas chromatograph Trace GC Ultra coupled to an ion-trap mass spectrometer ITQ 900, Thermo Scientific) to determine the chemical components and their respective percentage. The components were separated on a non-polar capillary column ZB5 (Phenomenex) in a temperature program 60–320 °C with a gradient of 4 °C min<sup>-1</sup>. Identification of molecular components was established by comparing mass spectra with the NIST library and by verification of retention times for the highest score records.

TLE from dried needle samples was obtained using Soxhlet extraction in a mixture solution of 90% dichloromethane and 10% methanol (BECHTEL, 2018; FORNACE, 2014; FREIMUTH, 2017) for three types of samples: 1) needles without decomposition by the EL procedure (extract\_noEL), 2) needles after finishing the EL procedure without artificial ozonation (extract\_EL), and 3) needles after finishing the EL procedure additionally ozonated (extract\_ELO<sub>3</sub>). TLE from water leachates was extracted into hexane (20 ml hexane: 75 ml leachate) for samples without artificial ozonation (leachate\_EL) and ozonized (leachate\_ELO<sub>3</sub>). This experiment was performed on autumn samples of *P. mugo* needles.

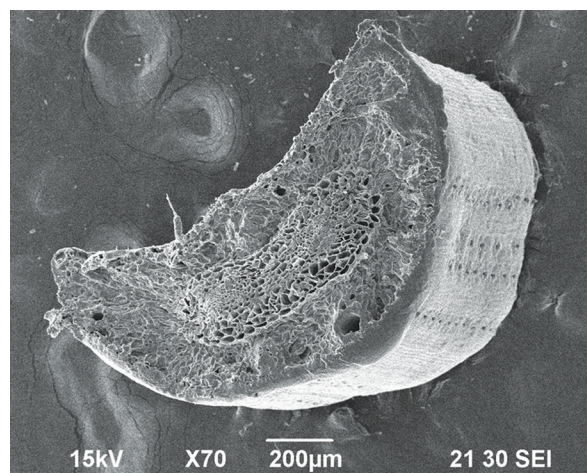


Fig. 6. Cross-section profile of *P. mugo* needle recorded by JEOL - Model JSM-6390 - Scanning Electron Microscope at Laboratory center of Earth Science Institute of SAS; accelerating voltage: 15 kV, magnification: 70×, resolution: 200 µm

### Oxidative stability

We defined the oxidative stability (OxS) as the median of differences between injury indices before and after additional artificial ozonation ( $OxS = INX - INXO_3$ ) for the group of samples gathered in single clusters considering for beginning and end of the growing season, separately. Indices INX (%) and INXO<sub>3</sub> (%) were converted from percentage to decimal format, therefore OxS ranges from -1 to 1, where OxS equal to 0 means that examined plant tissue is oxidatively stable, i.e. without any proven oxidative effect.  $OxS < 0$  indicates the rate of instability or sensitivity of plant tissue to oxidative stress. Plant tissues characterised by  $OxS > 0$  are considered resistant to oxidative stress with the positive effect of artificial ozonation. The paired t-test in software Statistica was used to test the differences between OxS of *P. mugo* needle samples gathered in June and October in individual years. The differences between OxS were considered significant when the null hypothesis of no differences between the samples was rejected at  $p < 0.05$  and indicate significant differences.

To validate the presented modified EL method, we applied the EL procedure on needle samples of different adult conifers growing under the same climate and environmental conditions at the foothill of the High Tatra Mts (locality of Stará Lesná, 49.15199°N, 20.28810°E, 810 m asl) in autumn 2020. Since the incorporated conifers differ by the needle structure and physiology, we expected divergent oxidative sensitivity between species.

### Modelling of ozone dose

Quantity of ozone dose up-taken by plant material in natural conditions was modelled by DO<sub>3</sub>SE model (EMBERSON et al., 2000; BÜKER et al., 2012; SEI, 2014) parametrized for *P. mugo* (BIČÁROVÁ et al., 2019). This model processed O<sub>3</sub> and meteorological input data (Table 2) measured at Skalnaté Pleso Observatory for the growing season defined from the 1<sup>st</sup> of June to the 30<sup>th</sup> of September. The

ambient O<sub>3</sub> concentrations were continuously monitored by Thermo Electron Environmental 49C device that works on the principle of UV absorption by O<sub>3</sub> at a wavelength of 254 nm.

Meteorological variables were recorded by a reliable measurement system based on a PROlog ultra-low-power datalogger (Physicus, SK). The measurement of ozone suggests high O<sub>3</sub> concentrations in the subalpine zone of the High Tatra Mts where our monitoring sites are situated. As demonstrated in Table 2, O<sub>3</sub> concentrations varied around 50 ppb, on average over the growing season. These values exceeded average O<sub>3</sub> concentrations referred to O<sub>3</sub> daily mean data (33.0 ppb) as well as O<sub>3</sub> daily maxima (42.6 ppb) derived from measurement at ground stations organized in the European air quality monitoring network (EMEP, 2020). In this work, the model output of phytotoxic ozone dose without threshold limitation ( $Y = 0$ ) i.e. POD<sub>0</sub> was considered identical to MO<sub>3</sub>D. Phytotoxicity of ozone dose was assessed according to relations of MO<sub>3</sub>D with VINO<sub>3</sub> and O<sub>x</sub>S.

## Results and discussion

### Electrolyte leakage

The obtained results confirmed the assumption about different levels of conductivity measured before (final conductivity – C<sub>f</sub>) and after (total conductivity – C<sub>t</sub>) total destruction of plant material (Fig. 7). The serious increase of electrolyte leakage from plant tissues of *P. mugo* needles to water solution was caused by extensive damage of cell membranes under autoclave conditions (point 7 of EL procedure description). C<sub>t</sub> varied mostly between 50 and 70 μS cm<sup>-1</sup> whereas C<sub>f</sub> was substantially lower, at the level of 25 μS cm<sup>-1</sup>. Additional oxidation under artificial ozonation may have caused that the level of C<sub>f</sub> for samples ozonized in the laboratory chamber was slightly higher when compared with those ozonized just by ambient ozone in the natural conditions. We assume that these small differences in C<sub>f</sub> between additionally ozonized and non-ozonized samples highlight the special natural protective function of *P. mugo* membrane cells, sufficient to defend against oxidative stress that occur in natural environment.

The degree of cell membrane damage expressed by injury indices is depicted in Figure 8. The injury index of the additionally non-ozonized group of samples (INX) shows the percentage of cell membrane damage on average 12% ± 3% which indicates minor injury caused by stress factors in natural environment. The intra-annual changes of INX show a decrease by 2–5% from June to October, which was not significant ( $p = 0.08$ , Table 3). Weakened tolerance to oxidative stress at the beginning of the growing season may be associated with the health state of needles after winter. The low snow depth and winter warm spells during winter cause the decrease of the greenness of dense *P. mugo* thickets particularly at the lower altitudes (LUKASOVÁ et al., 2021). During the loss of the insulation function of the snow cover, the climate-induced injury of

Table 2. Statistics of hourly O<sub>3</sub> and meteorological data measured at Skalnaté Pleso Obs. used in DO<sub>3</sub>SE model for simulation of ozone dose absorbed by *P. mugo* during growing season in 2019 and 2020

Variables	Statistics	*2019	*2020
O <sub>3</sub> concentration: O <sub>3</sub> (ppb)	Mean	52.50	49.00
	Max	90.30	70.50
	Min	27.80	23.00
	STD	8.30	7.40
Air temperature: AT (°C)	Mean	11.30	10.70
	Max	25.30	20.70
	Min	-2.90	0.10
	STD	4.50	3.70
Vapour pressure deficit: VPD (kPa)	Mean	0.26	0.19
	Max	1.89	1.17
	Min	0.00	0.00
	STD	0.25	0.21
Precipitation: P (mm)	Mean	0.19	0.26
	Sum	551.00	758.00
	Max	36.00	18.00
	STD	1.27	1.13
Global solar radiation: R (kW m <sup>-2</sup> )	Mean	0.18	0.16
	Sum	518.00	474.00
	Max	1.10	1.13
	STD	0.24	0.23

\*Period from 01/06 to 30/09.

shoots protruding above the snow surface or completely exposed after snow-melting suffers from the winter desiccation (WARDLE, 1981) and abrasion by wind-blown ice crystals (SONESSON and CALLAGHAN, 1991; WALKER et al., 2001). The incomplete snow cover leads to photoinhibition of the photosystem II (PSII), in higher water losses as well as lower dehydration tolerance because both osmotic adjustment and changes in turgor maintenance capacity are reduced (NEUNER et al., 1999). Symptoms of low temperature damage of the photosynthetic apparatus are particularly evident when substantial light intensity follows exposure to low-temperatures (GOH et al., 2012).

In all sample collections, INXO<sub>3</sub> reflecting the artificial ozonation were higher when compared with INX i.e. injury without additional ozonation (Fig. 8). The samples of *P. mugo* needles gathered in the same month showed significantly different injury indices depending on if they were additionally ozonized or not ( $p = 0.00$ , Table 3). Increase of injury from INX level of 12% and 14% to INXO<sub>3</sub> of 25% was achieved in June 2019 and 2020, respectively. Similarly, INXO<sub>3</sub> exceeded INX values in October for both years. INXO<sub>3</sub> shows also significant intra-annual differences between samples gathered in June and those from October ( $p = 0.00$ , Table 3). The lower INXO<sub>3</sub> in autumn compared to late spring indicates the ability of *P. mugo* to strengthen the resistance against the stress factors over the growing period. This improved tolerance may result from

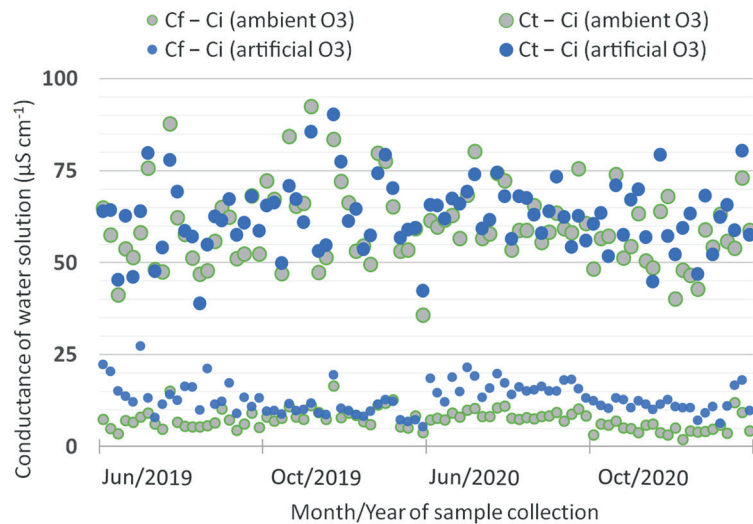


Fig. 7. Conductivity of water solution with leached *P. mugo* needle samples collected at monitoring sites S1–S10 in the High Tatra Mts at the start (Jun) and the end ( $O_{ct}$ ) of growing seasons 2019 and 2020. Small dots and large dots represent conductivity before ( $C_f-C_i$ ), and after ( $C_t-C_i$ ) autoclave destruction, respectively. Green dots show conductivity of samples exposed by ambient  $O_3$  in natural environment, blue dots represent conductivity of samples after additional ozonation in laboratory chamber.

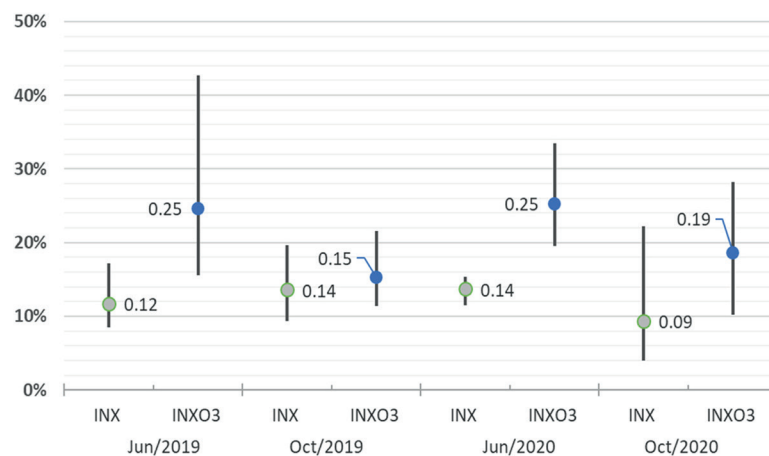


Fig. 8. Statistics (max, min, avg) of injury indices INX and  $INXO_3$  for *P. mugo* in the High Tatra Mts at the start (Jun) and the end (Oct) of growing seasons 2019 and 2020.

activation of antioxidant agents (KORMUŠÁK et al., 2019; MATĽOK et al., 2020), since the environmental factors such as air humidity and soil moisture conditions allow almost unlimited absorbance of  $O_3$  into conifer needle tissues (BIČÁROVÁ et al., 2019).

Table 3. Results of pair sampled t-test of injury index between additionally ozonized ( $INXO_3$ ) and non-ozonized (INX) samples of *P. mugo* needles gathered in June and October in 2019 and 2020; the significant differences with  $p < 0.05$  are in bold.

Differences in injury indices (INX a $INXO_3$ ) between samples:	p
INX and $INXO_3$ in June	<b>0.00</b>
INX and $INXO_3$ in October	<b>0.00</b>
$INXO_3$ in June and $INXO_3$ in October	<b>0.00</b>
INX in June and INX in October	0.08

### GC/MS analysis

Chemical components of total lipid extract determined by GC/MS laboratory technique suggest qualitative and quantitative changes in *P. mugo* samples after additional ozonation in both dried needle samples and EL leachates.

### TLE of dried needles

The chemical composition of TLE selected from dried needle samples after different EL procedures is shown in Figure 9. More detailed characteristics of GC/MS analysis are presented in Figure 10 and Table 4. The application of the EL method led to a decrease in the relative percentage of sesquiterpenes such as Caryophyllene, Germacrene D,  $\alpha$ -Muuroolene,  $\delta$ -Cadinene that naturally occur in plant tissues. Contrary, these substances dominated in noEL

samples. Effect of artificial ozonation could be documented by the formation of oxidative hydrocarbons derived from  $\delta$ -Cadinene including molecules of (-)-Spathulenol,  $\delta$ -Cadinol/tau.-Cadinol,  $\alpha$ -Cadinol and further oxidative forms such as Aminosalicic acid, n-Nonadecene\*, Hexadecanoic acid / FAME, sterol\*, Androstane derivative, 1-Naphthalenecarboxylic acid, 5-[2-(3-furanyl)ethyl]decahydro-1,4a-dimethyl-6-methylene-,methyl-ester,[1R-(1 $\alpha$ ,4 $\alpha$  $\beta$ ,5 $\beta$ ,8 $\alpha$ )], Podocarp-8(14)-en-15-oic acid, 13 $\beta$ -methyl-13-vinyl-, methyl ester. A higher percentage of these molecules was identified in ELO<sub>3</sub> compared to EL extracts. In EL extract,  $\alpha$ -Tocopherol (Vitamine E) was the highest percentage substance while in ELO<sub>3</sub> sample its content substantially decreased. We assume that was due to the contribution of the artificial ozone oxidative effect. Tocopherols inhibit the propagation of lipid peroxidation by scavenging lipid peroxy radicals and prevent lipid peroxidation by reacting with other reactive oxygen species, such as singlet oxygen, in cooperation with carotenoids (MUNNÉ-BOSCH, 2005).

#### TLE of needle leachates after completion of the EL procedure

GC/MS analysis revealed changes between leachates from needles after finishing the EL assay (Fig. 11, Fig. 12, Table 5). The effect of artificial ozone could be associated with oxidative decomposition of substances such as Isborneol,  $\alpha$ -Terpinyl acetate, Cyclohexane, (3-methylpentyl)-,1,7-Dimethyl-4-(1-methylethyl)cyclodecane,  $\delta$ -Cadinol. These substances were identified with higher percentage in EL leachate compared to ELO<sub>3</sub>. Contrary, the formation 3-Aminosalicic acid and Santalol/Lanceol with the high proportion in ELO<sub>3</sub> could be affected by the extreme oxidative environment during artificial ozonation.

#### Oxidative stability

Changes in oxidative stability of *P. mugo* needle tissue caused by artificial ozonation illustrates Figure 13. For all gathered sample sets, negative numbers of OxS varied near to the value of 0 which suggests relatively low sensitivity of *P. mugo* to oxidative stress induced by ozone. Our results show intra-annual OxS change characterised by moderate decrease of oxidative sensitivity from June to October in both years, 2019 and 2020. It is in contrast with expected oxidative damage of cell membranes due to effective stomatal O<sub>3</sub> flux into cell interiors. Analysing both years together, OxS of samples gathered in June significantly differ from OxS of samples in October ( $p = 0.00$ , Table 6). Furthermore, OxS of samples from individual years significantly differed ( $p = 0.01$ ), which was caused by the difference between samples from October 2019 and 2020 rather than balanced OxS of samples from June (Table 6). Since the tropospheric ozone is considered as an effective elicitor, which allows increasing content of bioactive compounds in pine shoots (MATLOK et al., 2020), a slight increase of OxS in October (Fig. 13) could relate to the activation of antioxidant enzymes in the needles acclimatised to increased levels of oxidative stress. Concentration of superoxide dismutase enzymes (SODs) typically increases with the degree of stress conditions. SODs act as antioxidants and protect cellular components from being oxidized when catalysing the production of O<sub>2</sub> and H<sub>2</sub>O<sub>2</sub> from superoxide (O<sub>2</sub><sup>-</sup>), (ALSCHER et al., 2002). KORMUŤAK et al. (2019) found increasing content of the SODs in the *P. mugo* needles in High Tatra Mts. from April, with the peak in August followed by a slow decrease until November. The essential oils, as well as the organic and hydroethanolic components in the fresh needles, can also play a key role in the antioxidant defence strategy of pine species

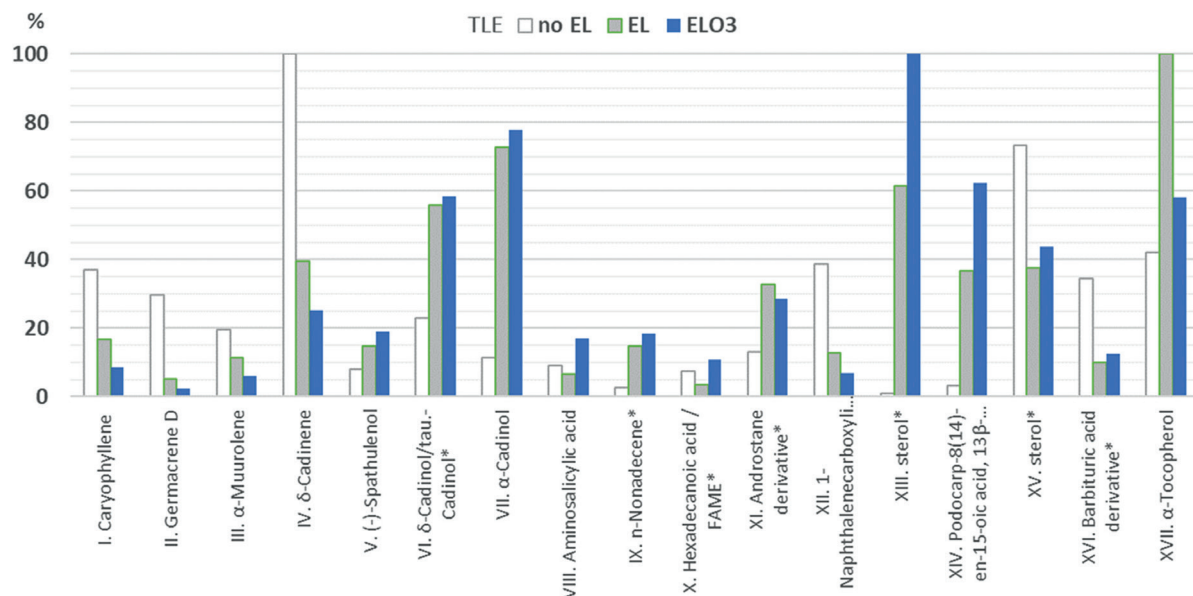


Fig. 9. Chemical composition of TLE samples of dried needles after different EL procedures; values on the y-axis are given as a percentage normalized to highest concentration compound; \*ambiguous identification of a compound.

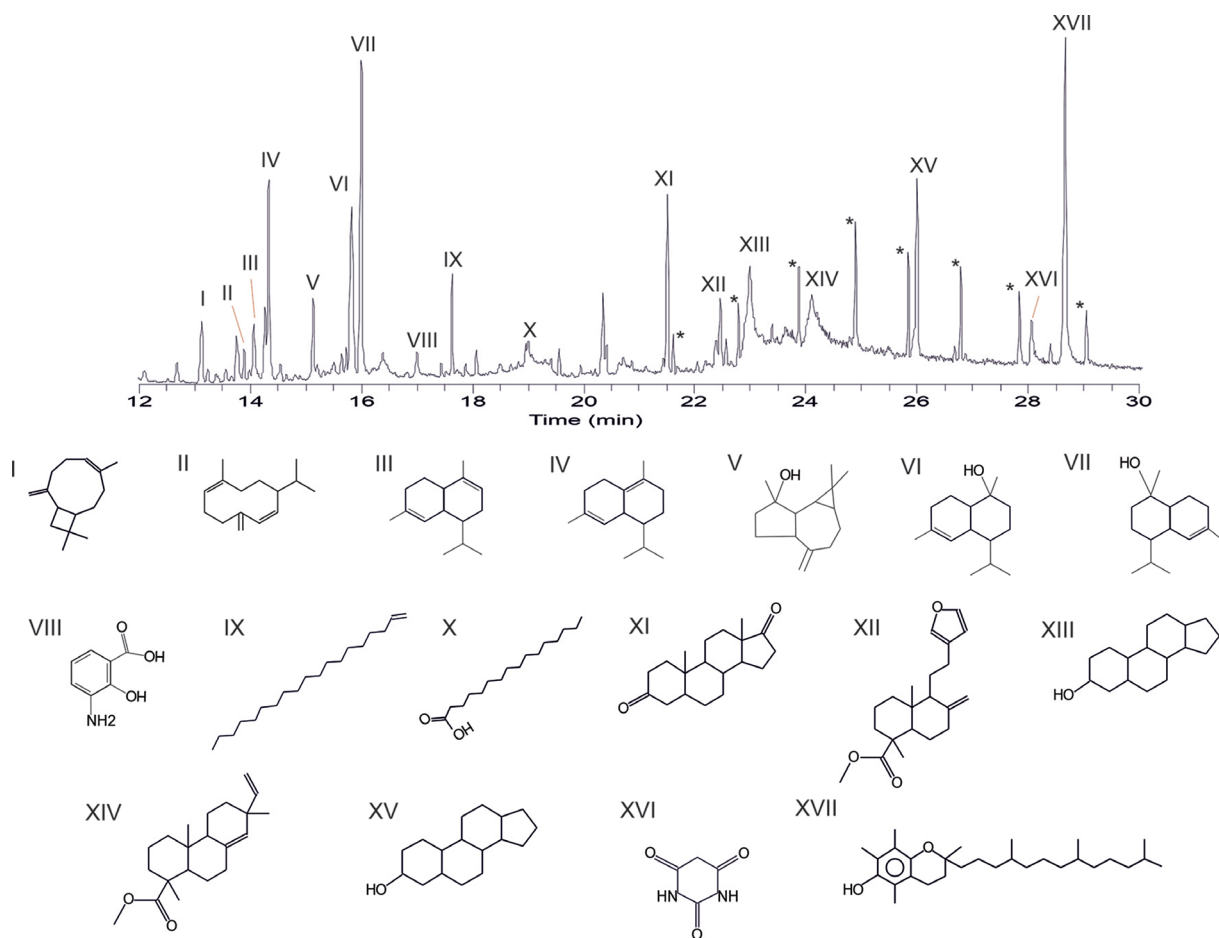


Fig. 10. GC chromatogram of TLE substances (\*peaks correspond to silicone contamination).

Table 4. Characteristics of substances identified in TLE. RI, retention index; \*ambiguous identification of a compound.

No.	Retention Index	No. CAS	Name
I	1449	87-44-5	Caryophyllene
II	1512	23986-74-5	Germacrene D
III	1527	10208-80-7	$\alpha$ -Muurolene
IV	1550	483-76-1	$\delta$ -Cadinene
V	1622	77171-55-2	(-)-Spathulenol
VI	1687	36564-42-8 /5937-11-1	$\delta$ -Cadinol/ $\tau$ au.-Cadinol*
VII	1703	481-34-5	$\alpha$ -Cadinol
VIII	1801	570-23-0	Aminosalicylic acid
IX	1865		<i>n</i> -Nonadecene*
X	2011		Hexadecanoic acid / FAME*
XI	2294		Androstane derivative*
XII	2412	10267-15-9	1-Naphthalenecarboxylic acid, 5-[2-(3-furanyl)ethyl] decahydro-1,4a-dimethyl-6-methylene-, methyl ester, [1R-(1 $\alpha$ ,4 $\alpha$ $\beta$ ,5 $\beta$ ,8 $\alpha$ )]-sterol*
XIII	2488		
XIV	2625	1686-54-0	Podocarp-8(14)-en-15-oic acid, 13 $\beta$ -methyl-13-vinyl-, methyl ester sterol*
XV	2870		
XVI	3161		Barbituric acid derivative*
XVII	3234	10191-41-0	$\alpha$ -Tocopherol

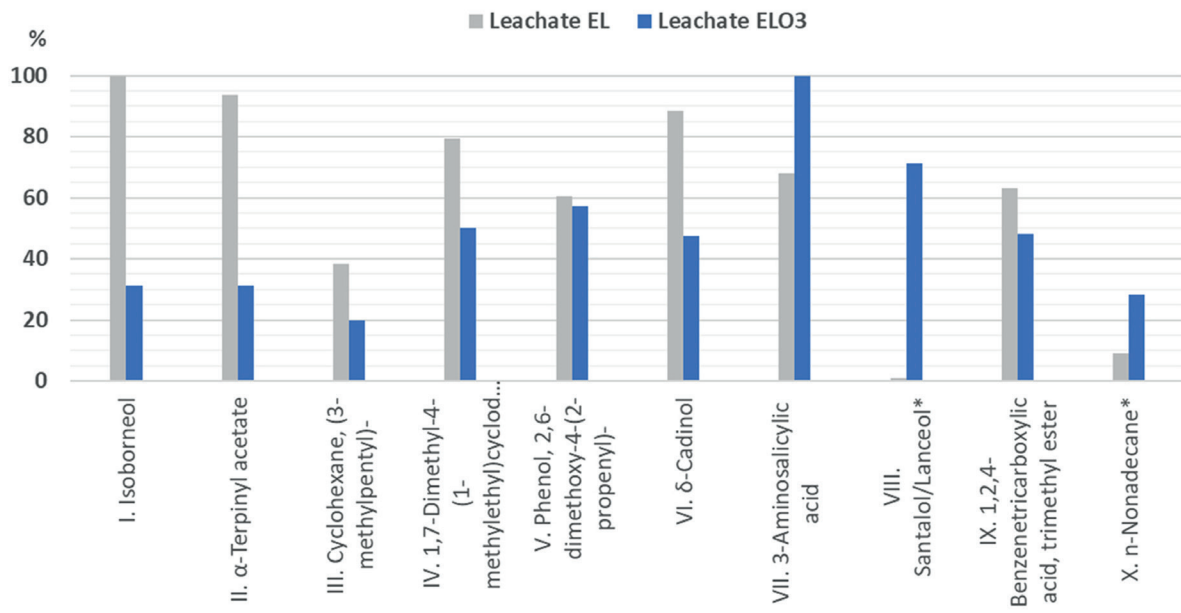


Fig. 11. Chemical composition of needle leachates for different EL procedures.

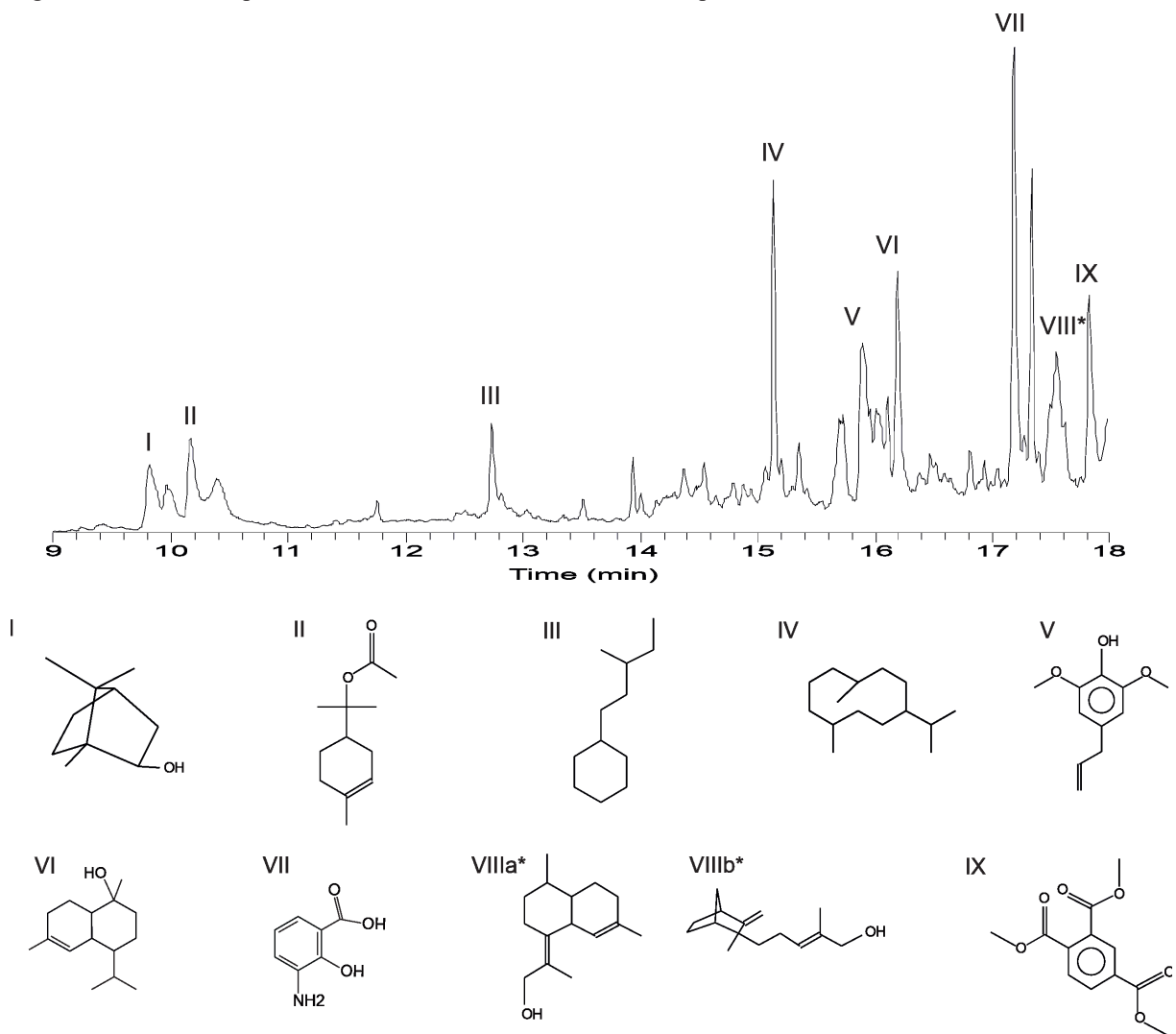


Fig. 12. GC chromatogram of leachate substances.

Table 5. Characteristics of substances in needle leachate after EL procedure

No.	Retention Index	No. CAS	Name
I	1211	124-76-5	Isoborneol
II	1232	80-26-2	$\alpha$ -Terpinyl acetate
III	1418	61142-38-9	Cyclohexane, (3-methylpentyl)-
IV	1621	645-10-3	1,7-Dimethyl-4-(1-methylethyl)cyclodecane
V	1693	6627-88-9	Phenol, 2,6-dimethoxy-4-(2-propenyl)-
VI	1719	36564-42-8	$\delta$ -Cadinol
VII	1817	570-23-0	3-Aminosalicylic acid
VIII	1857	10067-29-5	<i>Santalol/Lanceol*</i>
IX	1886	2459-10-1	1,2,4-Benzenetricarboxylic acid, trimethyl ester

(KOUTSAVITI et al., 2021). In addition, the increased tolerance to oxidative stress at the end of the growing season may be caused by autumn increase of the basic components of cellular membranes – phospholipids. An increased amount of phospholipids relate to the metabolic changes associated with the onset of winter dormancy, preparing the plants to low-temperature stress (PUKACKI, 2004).

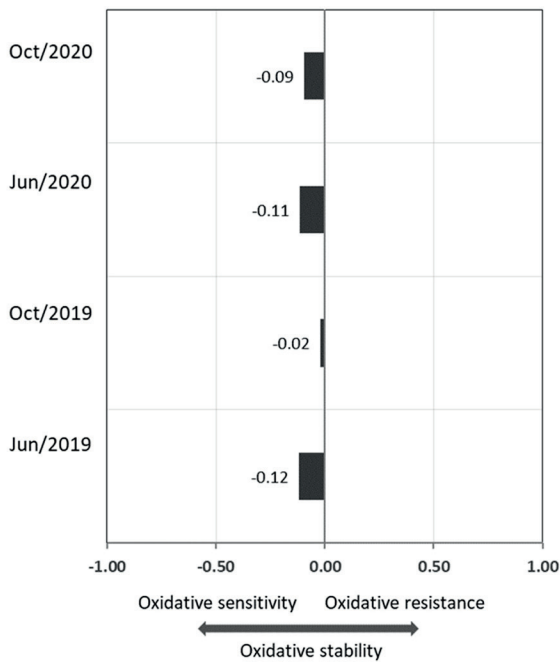


Fig. 13. Oxidative stability (OxS) of *P. mugo* in the High Tatra Mts using modified electrolyte leakage method; presented OxS values correspond to the median of the difference between injury indices INX and INXO<sub>3</sub> for a group of samples belonging to each collection term individually.

Table 6. Results of pair sampled t-test between oxidative stability (OxS) of *P. mugo* needle samples gathered in June and October in 2019 and 2020; the significant differences with  $p < 0.05$  are in bold.

Differences in oxidative stability (OxS) between samples:	P
2019 and 2020	<b>0.01</b>
June and October	<b>0.00</b>
June 2019 and June 2020	0.50
October 2019 and October 2020	<b>0.00</b>

The validation of EL method, which was realized in autumn 2020 on different conifer species growing at the foothill of the High Tatra Mts confirmed that this method is applicable for the quantification of oxidative stability of cell membranes. The validation revealed that the conifer species growing under the same climate and environmental conditions have different oxidative stability. Although the injury index of non-ozonized samples of all species was similar, the artificial ozonation led to the enhanced destruction of cell structures in Silver fir (*Abies alba*) and Norway spruce (*Picea abies*) needle samples (Table 7). Silver fir with the lowest OxS was the most sensitive species to ozone-induced stress followed by Norway spruce. Contrary, the pine species (*P. mugo*, *P. cembra*, and *P. sylvestris*) were revealed as relatively ozone-resistant.

Table 7. Sensitivity of different conifer tree species to artificial ozonation

Conifer type	INX	INXO <sub>3</sub>	OxS
Silver fir ( <i>Abies alba</i> )	0.14	0.67	-0.53
Norway spruce ( <i>Picea abies</i> )	0.09	0.42	-0.32
Mountain pine ( <i>P.mugo</i> )	0.17	0.33	-0.16
Swiss pine ( <i>P. cembra</i> )	0.16	0.26	-0.10
Scots pine ( <i>P. sylvestris</i> )	0.19	0.24	-0.06

### Visible foliar injury

As shown in Table 8, medians of VIN score observed on *P. mugo* needle (C + 2) samples for different type of harmful agents VINbio, VINabio, VINO<sub>3</sub> varied between 0 (no injury) and 2 (moderate injury). At the start of the growing season after the snow melt, minimal abiotic mechanical damage was observed (VINabio = 0). It is probably related to the protective function of the snow cover in winter. Deteriorated of VINabio from level 0 to 1 was recorded only during the growing season 2019. On the other hand, biotic injury factors were most pronounced in each of the collected groups of samples. Increase of VINbio from low (June) to moderate (October) injury was due to intensified harmful effect of insects, spider mites, and fungal diseases during summer. VINO<sub>3</sub> which represents the incidence of O<sub>3</sub> induced injury symptoms was stable at low level. Results of VINO<sub>3</sub> indicate a minor O<sub>3</sub> effect on *P. mugo* that is in good agreement with OxS values (Fig. 13). It could be

associated with SOD activity (ALSCHER et al., 2002) when the overproduction of SOD in the chloroplasts may result in a 3–4 fold reduction of visible O<sub>3</sub> injury (VAN CAMP et al., 1994).

### Modelled ozone dose

Figure 14 (left) illustrates the increment of MO<sub>3</sub>D from June to October and the cumulative amount of O<sub>3</sub> concentration measured in the natural environment for the same period. As we expected, this cumulative O<sub>3</sub> amount achieved a level of 150 ppm which corresponds to the level of O<sub>3</sub> amount in the laboratory chamber during the artificial ozonation of needle samples. Results of MO<sub>3</sub>D varied around a level of 15 mmol m<sup>-2</sup> for considering growing season. Higher MO<sub>3</sub>D in 2019 was probably related to the higher O<sub>3</sub> concentration in warmer and sufficiently humid weather (Table 2) that supports the stomatal O<sub>3</sub> flux into *P. mugo* plant cells. The seasonal courses of MO<sub>3</sub>D (Fig. 14 right) show a considerable increase in O<sub>3</sub> uptakes during June, July and August. During this time period, limitation of stomatal O<sub>3</sub> flux into plant material due to environmental factors was minimal. Assessment of the phytotoxic effect of MO<sub>3</sub>D in association with VINO<sub>3</sub> and OxS can

be useful in comprehensive analysis of plant's biological response of conifer tree to oxidative stress as well as other biological and abiological stress factors. The role of the epidemiological approach in the assessment of forest vegetation response to ozone impact is emphasized by SICARD et al. (2016). With respect to achieved results of VINO<sub>3</sub> (Table 8) and OxS (Fig. 13) we suggest considering MO<sub>3</sub>D in a range between 14–16 mmol m<sup>-2</sup> (Fig. 14) for the vegetation period (June–October) as ozone dose with minor phytotoxic effect on *P. mugo* growing in the subalpine zone in the High Tatra Mts.

### Conclusions

Our results demonstrate the application of the modified electrolyte leakage method to test the oxidative stability of conifer needle samples. Based on this method, we indicated moderate changes in the oxidative stability for *P. mugo* needle samples analysed at the beginning (June) and end (October) of the 2019 and 2020 growing seasons. We concluded that *P. mugo* was more sensitive to oxidative stress after cold winter than after warm summer. The slight improvement of oxidative tolerance at the end of vegeta-

Table 8. The score of visible injury (VIN) observed on the surface of *P. mugo* needle samples for biotic, abiotic, and O<sub>3</sub>-induced symptoms; the range of score from 0 (no injury) to 3 (extensively damage) is defined in Table 1. VINbio, VINabio, VINO<sub>3</sub> were derived as median of scores for each type of symptoms individually.

Sample number	VIN Jun/2019			VIN Oct/2019			VIN Jun/2020			VIN Oct/2020		
	bio	abio	O <sub>3</sub>									
S1/1	1	0	0	1	1	0	1	0	0	1	0	1
S1/2	0	0	1	1	1	0	1	0	1	1	0	2
S1/3	1	0	0	2	1	0	1	0	1	1	0	2
S2/1	1	0	0	1	1	0	1	0	1	1	1	1
S2/2	2	0	1	2	2	0	1	0	0	1	0	1
S2/3	2	0	2	1	1	0	2	0	0	2	0	2
S3/1	1	0	1	1	2	1	1	0	1	2	0	1
S3/2	1	0	0	1	1	1	1	0	1	1	0	1
S3/3	2	0	1	2	2	1	2	0	1	2	0	2
S4/1	2	0	1	2	2	1	2	0	1	2	0	2
S4/2	2	0	0	2	2	1	2	0	2	2	0	1
S4/3	2	0	2	2	3	2	2	0	1	2	0	1
S5/1	1	0	1	2	1	1	1	1	1	2	1	2
S5/2	2	0	0	2	1	2	1	1	1	2	0	2
S5/3	2	0	1	2	1	2	1	0	1	2	1	1
S6/1	1	0	0	2	1	1	1	0	1	2	0	1
S6/2	3	0	0	1	1	0	1	0	1	2	1	2
S6/3	1	0	1	1	1	0	1	1	1	1	0	1
S7	2	0	1	1	1	1	1	0	1	1	0	1
S8	1	2	1	1	1	1	1	0	1	1	0	2
S9	1	0	1	2	1	1	1	1	1	2	1	1
S10	2	0	1	2	2	2	1	1	1	2	1	2
Median	1.5	0.0	1.0	2.0	1.0	1.0	1.0	0.0	1.0	2.0	0.0	1.0

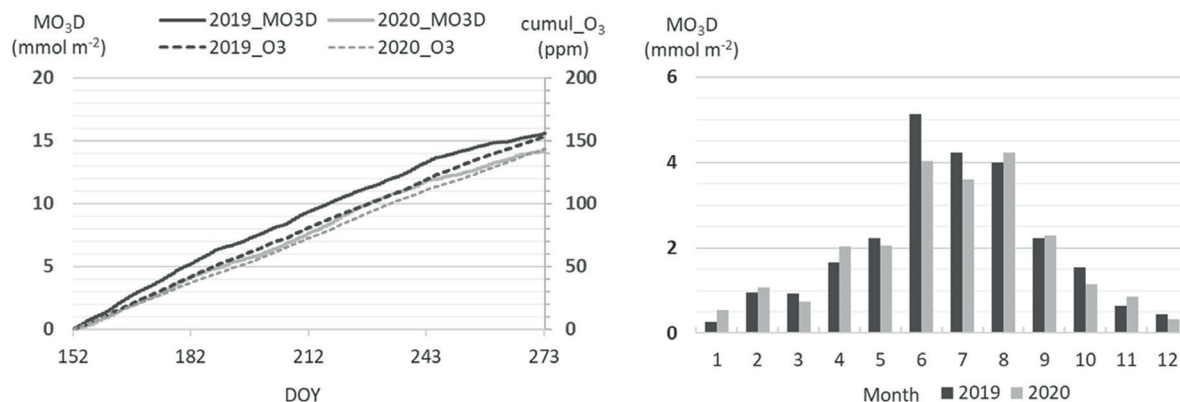


Fig. 14. The cumulative amount of measured O<sub>3</sub> concentration (cumul\_O<sub>3</sub>) and modelled ozone dose (MO<sub>3</sub>D) based on DO<sub>3</sub>SE model simulation of stomatal O<sub>3</sub> uptake to *P. mugo* in the natural environment of High Tatra Mts during the growing season (left) and all months (right) for the years 2019 and 2020.

tion season may be related to the effective activation of the antioxidant defence system during the warm months. GC/MS analysis confirmed qualitative and quantitative changes of chemical composition in needle samples after the application of artificial ozone. Compared with the other conifers (*Abies alba*, *Picea abies*), the pine species (*P. mugo*, *P. cembra*, and *P. sylvestris*) were revealed as relatively ozone-resistant. Visible inspection of O<sub>3</sub> symptoms, fungal diseases, biting insects, spider mites, and other tissue injuries showed the prevalence of biological harmful agents. Ozone-induced injury observed on the surface of 2-year-old needles was mostly low, characterised by the median score at level 1, i.e. affected surface in range between 1–5%. This damage was linked to MO<sub>3</sub>D values of 15.6 and 14.1 mmol m<sup>-2</sup> for the growing season 2019 and 2020, respectively. The phytotoxic effect of MO<sub>3</sub>D related to present results of oxidative stability and visible injury inspection may be classified as minor. We assume that OxS could be a complementary bio-chemical indicator to VINO<sub>3</sub> for appraisal of MO<sub>3</sub>D phytotoxicity as well as for the complex evaluation of all biotic and abiotic agents operating in the natural environment.

### Acknowledgements

This work was supported by the Scientific Grant Agency of the Slovak Republic, VEGA project 2/0093/21. We are grateful to all members of the technical staff of the Earth Science Institute of the Slovak Academy of Science and Slovak Hydrometeorological Institute for the data they measure at Skalnaté Pleso Observatory.

### List of abbreviations

C <sub>i</sub>	ultra-pure water conductivity at initial conditions
C <sub>f</sub>	final conductivity of water solution after non-destructive incubation of plant material
C <sub>t</sub>	total conductivity of water solution after total

C + 2	plant material destruction
DO <sub>3</sub> SE	2-year-old old needles
EL	deposition model for estimation of ozone dose up-taken by plant
GC/MS)	electrolyte leakage
MO <sub>3</sub> D	gas chromatography/mass spectrometry analysis
OxS	modelled ozone dose
VIN	oxidative stability
VINbio	visible injury
VINabio	visible injury due to biotic harmful agents (fungi, spider, insects)
VINO <sub>3</sub>	visible injury due to abiotic/mechanical effect
INX	visible injury induced by ambient ozone
INXO <sub>3</sub>	injury index related to ambient O <sub>3</sub> in real environment
	injury index related to effect of additional artificial ozonation

### References

- ALSCHER, R.G., ERTURK, N., HEATH, L.S., 2002. Role of superoxide dismutase (SODs) in controlling oxidative stress in plants. *Journal of Experimental Botany*, 53: 1331–1341. <https://doi.org/10.1093/jexbot/53.372.1331>
- BADEA, O., TANASE, M., GEORGETA, J., ANISOARA, L., PEIOV, A., UHLIROVA, H., PAJTIK, J., WAWRZONIAK, J., SHPARYK, Y., 2004. Forest health status in the Carpathian Mountains over the period 1997–2001. *Environmental Pollution*, 130: 93–98. <https://doi.org/10.1016/j.envpol.2003.10.024>
- BAJJI, M., KINET, J.M., LUTTS, S., 2002. The use of the electrolyte leakage method for assessing cell membrane stability as a water stress tolerance test in durum wheat. *Plant Growth Regulation*, 36: 61–70. <https://doi.org/10.1023/A:1014732714549>
- BALLIAN, D., RAVAZZI, C., DE RIGO, D., CAUDULLO, G., 2016. *Pinus mugo* in Europe: distribution, habitat, usage and threats. In SAN-MIGUEL-AYANZ, J., DE RIGO, D., CAUDULLO, G., HOUSTON DURRANT, T., MAURI, A. (eds). *European atlas of forest tree species*. [online]. [cit. 2022-08-11]. Luxembourg: Publications Office of the European Union,

- p. 125. <https://data.europa.eu/doi/10.2760/776635>
- BECHTEL, A., OBERAUER, K., KOSTIĆ A., GRATZER, R., MILISAVLJEVIĆ, V., ALEKSIĆ, N., STOJANOVIĆ, K., GROSS, D., SACHSENHOFER, R.F., 2018. Depositional environment and hydrocarbon source potential of the Lower Miocene oil shale deposit in the Aleksinac Basin (Serbia). *Organic Geochemistry*, 115: 93–112. <https://doi.org/10.1016/j.orggeochem.2017.10.009>
- BELL, M.D., FELKER-QUINN, E., KOHUT, R., 2020. *Ozone sensitive plant species on National Park Service lands*. [online]. [cit. 2022-08-08]. Natural Resource Report NPS/WASO/NRR—2020/2062. Colorado: U.S. Department of the Interior, National Park Service, Natural Resource Stewardship and Science. <https://irma.nps.gov/DataStore/DownloadFile/636658>
- BIČÁROVÁ, S., SITKOVÁ, Z., PAVLENDOVÁ, H., FLEISCHER, P. JR., FLEISCHER, P., BYTNEROWICZ, A., 2019. The role of environmental factors in ozone uptake of *Pinus mugo* Turra. *Atmospheric Pollution Research*, 10: 283–293. <https://doi.org/10.1016/j.apr.2018.08.003>
- BORATYŃSKI, A., JASIŃSKA, A., BORATYŃSKA, K., ISZKULO, G., PIORKOWSKA, M., 2009. Life span of needles of *Pinus mugo* Turra: effect of altitude and species origin. *Polish Journal of Ecology*, 57: 567–572.
- BRAUN, S., SCHINDLER, C., RIHM, B., 2017. Growth trends of beech and Norway spruce in Switzerland: The role of nitrogen deposition, ozone, mineral nutrition and climate. *Science of The Total Environment*, 599–600: 637–646. <https://doi.org/10.1016/j.scitotenv.2017.04.230>
- BÜKER, P., MORRISSEY, T., BRIOLAT, A., FALK, R., SIMPSON, D., TUOVINEN, J.-P., ALONSO, R., BARTH, S., BAUMGARTEN, M., GRULKE, N., KARLSSON, P.E., KING, J., LAGERGREN, F., MATYSSEK, R., NUNN, A., OGAYA, R., PEÑUELAS, J., RHEA, L., SCHAUB, M., UDDLING, J., WERNER, W., EMBERSON, L.D., 2012. DO<sub>3</sub>SE modelling of soil moisture to determine ozone flux to forest trees. *Atmospheric Chemistry and Physics*, 12: 5537–5562. <https://doi.org/10.5194/acp-12-5537-2012>
- BYTNEROWICZ, A., FENN, M.E., CISNEROS, R., SCHWEIZER, D., BURLEY, J., SCHILLING, S.L., 2019. Nitrogenous air pollutants and ozone exposure in the central Sierra Nevada and White Mountains of California – Distribution and evaluation of ecological risks. *Science of the Total Environment*, 654: 604–615. <https://doi.org/10.1016/j.scitotenv.2018.11.011>
- COULSTON, J.W., SMITH, G.C., SMITH, W.D., 2003. Regional assessment of ozone sensitive tree species using bioindicator plants. *Environmental Monitoring and Assessment*, 83: 113–127. <http://doi.org/10.1023/A:1022578506736>
- DALSTEIN, L., CIRIANI, M.L., 2019. Ozone foliar damage and defoliation monitoring of *P. cembra* between 2000 and 2016 in the southeast of France. *Environmental Pollution*, 244: 451–461. <https://doi.org/10.1016/j.envpol.2018.10.081>
- DEMIDCHIK, V., STRALTSOVA, D., MEDVEDEV, S., POZHVANOV, G.-A., SOKOLIK, A., YURIN, V., 2014. Stress-induced electrolyte leakage: the role of K<sup>+</sup>-permeable channels and involvement in programmed cell death and metabolic adjustment. *Journal of Experimental Botany*, 65: 1259–1270. <https://doi.org/10.1093/jxb/eru004>
- EMBERSON, L.D., ASHMORE, M.R., CAMBRIDGE, H.M., SIMPSON, D., TUOVINEN, J.P., 2000. Modelling stomatal ozone flux across Europe. *Environmental Pollution*, 109: 403–413. [http://doi.org/10.1016/S0269-7491\(00\)00043-9](http://doi.org/10.1016/S0269-7491(00)00043-9)
- EMEP, 2020. *Transboundary particulate matter, photo-oxidants, acidifying and eutrophying components. Status Report 1/2020*. [online]. [cit. 2022–09–06]. Oslo: Norwegian Meteorological Institute. [https://emep.int/publ/reports/2020/EMEP\\_Status\\_Report\\_1\\_2020.pdf](https://emep.int/publ/reports/2020/EMEP_Status_Report_1_2020.pdf)
- ESCANDÓN, M., CAÑAL, M.J., PASCUAL, J., PINTO, G., CORREIA, B., AMARAL, J., MEIJÓN, M., 2016. Integrated physiological and hormonal profile of heat-induced thermotolerance in *Pinus radiata*. *Tree Physiology*, 36: 63–77. <https://doi.org/10.1093/treephys/tpv127>
- FLEISCHER, P., PICHLER, V., FLEISCHER, P. JR., HOLKO, L., MÁLIŠ, F.G., GÖMÖRYOVÁ, E., CUDLÍN, P., HOLEKSA, J., MICHALKOVÁ, Z., HOMOLOVÁ, Z., ŠKVARENINA, J., STŘELCOVÁ, K., HLAVÁČ, P., 2017. Forest ecosystem services affected by natural disturbances, climate and land-use changes in the Tatra Mountains. *Climate Research*, 73: 57–71. <http://dx.doi.org/10.3354/cr01461>
- FLINT, H.L., BOYCE, B.R., BEATTIE, D.J., 1967. Index of injury—a useful expression of freezing injury to plant tissues as determined by the electrolytic method. *Canadian Journal of Plant Sciences*, 47: 229–230. <https://doi.org/10.4141/cjps67-043>
- FORNACE, K.L., HUGHEN, K.A., SHANAHAN, T.M., FRITZ, S.C., BAKER, P.A., SYLVA, S.P., 2014. A 60,000-year record of hydrologic variability in the Central Andes from the hydrogen isotopic composition of leaf waxes in Lake Titicaca sediments. *Earth and Planetary Science Letters*, 408: 263–271. <http://doi.org/10.1016/j.epsl.2014.10.024>
- FREIMUTH, E.J., DIEFENDORF, A.F., LOWELL, T.V., 2017. Hydrogen isotopes of n-alkanes and n-alkanoic acids as tracers of precipitation in a temperate forest and implications for paleorecords. *Geochimica et Cosmochimica Acta*, 206: 166–183. <http://dx.doi.org/10.1016/j.gca.2017.02.027>
- FURT, F., SIMON-PLAS, F., MONGRAND, S., 2011. Lipids of the Plant Plasma Membrane. In MURPHY, A., SCHULZ, B., PEER, W. (eds). *The plant plasma membrane*. Plant Cell Monographs, Volume 19. Berlin: Springer, p. 3–30. [https://doi.org/10.1007/978-3-642-13431-9\\_1](https://doi.org/10.1007/978-3-642-13431-9_1)
- GOH, C.-H., KO, S.-M., KOH, S., KIM, Y.-J., BAE, H.-J., 2012. Photosynthesis and environments: photoinhibition and repair mechanisms in plants. *Journal of Plant Biology*, 55: 93–101. <https://doi.org/10.1007/s12374-011-9195-2>
- HŮNOVÁ, I., KURFÜRST, P., BALÁKOVÁ, L., 2019. Areas under high ozone and nitrogen loads are spatially disjunct in Czech forests. *Science of The Total Environment*, 656: 567–575. <https://doi.org/10.1016/j.scitotenv.2018.11.371>
- ICP, 2014. *Examples of ozone damage in trees*. [online]. [cit. 2022–07–029]. Bangor: UK Centre for Ecology & Hydrology <https://icpvegetation.ceh.ac.uk/>
- KOPÁČEK, J., KAŇA, J., BIČÁROVÁ, S., FERNANDEZ, I., HEJZLAR, J., KAHOUNOVÁ, M., NORTON, S.A., STUHLÍK, E., 2017. Climate change increasing calcium and magnesium leaching from granitic Alpine catchments. *Environmental Science and Technology*, 51: 159–166. <https://doi.org/10.1021/acs.est.6b03575>
- KORMUŤÁK, A., GALGÓCI, M., BOLEČEK, P., GÖMÖRY, D., 2019. Antioxidant enzyme activity in *Pinus mugo* Turra, *P. sylvestris* L. and in their putative hybrids. *Biologia*, 74: 631–638. <https://doi.org/10.2478/s11756-019-00198-y>
- KOUTSAVITI, A., TOUTOUNGY, S., SALIBA, R., LOUPASSAKI, S., TZAKOU, O., ROUSSIS, V., IOANNOU, E., 2021. Antioxidant potential of pine needles: a systematic study on the

- essential oils and extracts of 46 species of the genus *Pinus*. *Foods*, 10: 2304–8158. <https://doi.org/10.3390/foods10010142>
- LEE, B., ZHU, J.K., 2010. Phenotypic analysis of Arabidopsis mutants: electrolyte leakage after freezing stress. *Cold Spring Harbor Protocols*, 2010: pdb.prot4970. <https://doi.org/10.1101/pdb.prot4970>
- LEVITT, J. (ed.), 1972. *Responses of plants to environmental stresses*. New York: Academic Press.
- LICHTENTHALER, K., 1996. Vegetation stress: an introduction to the stress concept in plants. *Journal of Plant Physiology*, 148: 4–14. [https://doi.org/10.1016/S0176-1617\(96\)80287-2](https://doi.org/10.1016/S0176-1617(96)80287-2)
- LUKASOVÁ, V., BUCHA, T., MAREKOVÁ, L., BUCHHOLCEROVÁ, A., BIČÁROVÁ, S., 2021. Changes in the greenness of mountain pine (*Pinus mugo* Turra) in the subalpine zone related to the winter climate. *Remote Sensing*, 13: 1788. <https://doi.org/10.3390/rs13091788>
- MATŁOK, N., GORZELANY, J., PIECHOWIAK, T., ANTOS, P., ZARDZEWIĄŁY, M., BALAJEJDER, M., 2020. Impact of ozonation process on the content of bioactive compounds with antioxidant properties in Scots pine (*L.*) shoots as well as yield and composition of essential oils. *Acta Universitatis Cibiniensis. Series E: Food Technology*, 24: 146–155. <https://doi.org/10.2478/auft-2020-0013>
- MEZEI, P., JAKUŠ, R., PENNERSTORFER, J., HAVAŠOVÁ, M., ŠKVARENINA, J., FERENČÍK, J., SLIVINSKÝ, J., BIČÁROVÁ, S., BILČÍK, D., BLAŽENEC, M., NETHERER, S., 2017. Storms, temperature maxima and the Eurasian spruce bark beetle *Ips typographus*—An infernal trio in Norway spruce forests of the Central European High Tatra Mountains. *Agricultural and Forest Meteorology*, 242: 85–95. <https://doi.org/10.1016/j.agrformet.2017.04.004>
- MUNNÉ-BOSCH S., 2005. The role of alpha-tocopherol in plant stress tolerance. *Journal of Plant Physiology*, 162: 743–748. <https://doi.org/10.1016/j.jplph.2005.04.022>
- NEUNER, G., AMBACH, D., AICHNER, K., 1999. Impact of snow cover on photoinhibition and winter desiccation in evergreen *Rhododendron ferrugineum* leaves during subalpine winter. *Tree Physiology*, 19: 725–732. <https://doi.org/10.1093/treephys/19.11.725>
- NUNN, A.J., WIESER, G., METZGER, U., LÖW, M., WIPFLER, P., HÄBERLE, K.-H., MATYSSEK, R., 2007. Exemplifying whole-plant ozone uptake in adult forest trees of contrasting species and site conditions. *Environmental Pollution*, 146: 629–639. <https://doi.org/10.1016/j.envpol.2006.06.015>
- PENNAZIO, S., SAPETTI, C., 1982. Electrolyte leakage in relation to viral and abiotic stresses inducing necrosis in cowpea leaves. *Biologia Plantarum*, 24: 218–225. <https://doi.org/10.1007/BF02883667>
- PUKACKI, P., 2004. The effect of industrial air pollution on membrane lipid composition of Scots pine (*Pinus sylvestris* L.) needles. *Acta Societatis Botanicorum Poloniae*, 73: 187–191. <http://dx.doi.org/10.5586/asbp.2004.025>
- SALEEM, S., BARI, A., ABID, B., TAHIR UL QAMAR, M., ATIF, R.M., KHAN, M.S., 2020. QTL Mapping for abiotic stresses in cereals. In FAHAD, S., HASANUZZAMAN, M., ALAM, M., ULLAH, H., SAEED, M., ALI KHAN, I., ADNAN, M. (eds). *Environment, climate, plant and vegetation growth*. Cham: Springer. 686 p. [https://doi.org/10.1007/978-3-030-49732-3\\_10](https://doi.org/10.1007/978-3-030-49732-3_10)
- SEI, 2014.  $\text{DO}_3\text{SE}$  (*Deposition of ozone for stomatal exchange*). [online]. [cit. 2022–07–15]. Stockholm: Stockholm Environment Institute. <https://www.sei-international.org/do3se>
- SCHAUB, M., CALATAYUD, V., FERRETTI, M., BRUNIALTI, G., LÖVBLAD, G., KRAUSE, G., SANZ, M.J 2016. Part VIII: Monitoring of ozone injury. In UNECE ICP Forests Programme Co-ordinating Centre (ed.). *Manual on methods and criteria for harmonized sampling, assessment, monitoring and analysis of the effects of air pollution on forests*. Thünen Institute of Forest Ecosystems. [online]. [cit.2022-08-25]. 14 p.[https://www.icp-forests.org/pdf/manual/2016/ICP\\_Manual\\_2016\\_01\\_part08.pdf](https://www.icp-forests.org/pdf/manual/2016/ICP_Manual_2016_01_part08.pdf)
- SHARPS, K., MILLS, G., HARMENS, H., 2014. *Have you seen these ozone injury symptoms?* [online]. [cit. 2022-08-19]. Bangor: UK Centre for Ecology and Hydrology. <https://icpvegetation.ceh.ac.uk/>
- SICARD, P., DE MARCO, A., DALSTEIN-RICHIER, L., TAGLIAFERRO, F., RENOU, C., PAOLETTI, E., 2016. An epidemiological assessment of stomatal ozone flux-based critical levels for visible ozone injury in Southern European forests. *Science of The Total Environment*, 541: 729–741. <http://doi.org/10.1016/j.scitotenv.2015.09.113>
- SONESSON, M., CALLAGHAN, T., 1991. Strategies of survival in plants of the Fennoscandian tundra. [online]. [2022-07-22]. *Arctic*, 42: 95–105. [www.jstor.org/stable/40511069](http://www.jstor.org/stable/40511069)
- VAN CAMP, W., WILLEKENS, H., BOWLER, C., VAN MONTAGU, M., INZÉ, D., REUPOLD-POPP, P., SANDERMANN, H. JR., LANGEBAEELS, C., 1994. Elevated levels of superoxide dismutase protect transgenic plants against ozone damage. *Nature Biotechnology*, 12: 165–168. <https://doi.org/10.1038/nbt0294-165>
- WALKER, D., BILLINGS, W., DE MOLENAAR, J., 2001. Snow-vegetation interactions in tundra environments. In JONES, H., POMEROY, J., WALKER, D., HOHAM, R. (eds.). *Snow Ecology: an interdisciplinary examination of snow-covered ecosystems*. [online]. [cit. 2022-08-25]. Cambridge: Cambridge University Press, p. 266–324. <https://www.nhbs.com/snow-ecology-book>
- WARDLE, P., 1981. Winter desiccation of conifer needles simulated by artificial freezing. *Arctic and Alpine Research*, 13: 419–423.
- YALCINKAYA, T., UZILDAY, B., OZGUR, R., TURKAN, I., MANO, J., 2019. Lipid peroxidation-derived reactive carbonyl species (RCS): their interaction with ROS and cellular redox during environmental stresses. *Environmental and Experimental Botany*, 165: 139–149. <https://doi.org/10.1016/j.envexpbot.2019.06.004>
- ZAPLETAL, M., PRETEL, J., CHROUST, P., CUDLÍN, P., EDWARDS-JONÁŠOVÁ, M., URBAN, O., POKORNÝ, R., CZERNÝ, R., HŮNOVÁ, I., 2012. The influence of climate change on stomatal ozone flux to a mountain Norway spruce forest. *Environmental Pollution*, 169: 267–273. <https://doi.org/10.1016/j.envpol.2012.05.008>

Received September 12, 2022

Accepted November 7, 2022